Journal of Colloid and Interface Science 570 (2020) 109–115

Contents lists available at ScienceDirect

Journal of Colloid and Interface Science

journal homepage: www.elsevier.com/locate/jcis

Elucidating the role of electrophoretic mobility for increasing yield in the electrophoretic deposition of nanomaterials

Prabal Tiwari, Noah D. Ferson, Jennifer S. Andrew *

Department of Materials Science and Engineering, University of Florida, Gainesville, FL 32611, United States

GRAPHICAL ABSTRACT

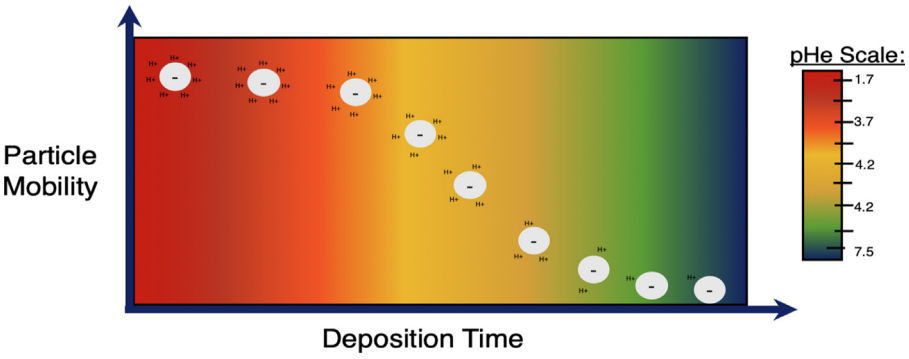

ARTICLE INFO

Article history:
Received 23 December 2019
Revised 25 February 2020
Accepted 25 February 2020
Available online 27 February 2020

Keywords:
Electrophoretic deposition
EPD
Alumina
Porous films
Nanoparticle films
Electrophoretic deposition kinetics
Particle mobility
Electrophoretic mobility
Scalable nanomanufacturing
Materials assembly

ABSTRACT

Hypothesis: Catalysts, chemical, gas, and bio- sensing devices fabricated from porous nanoparticle films show better performance and sensitivity than their bulk material counterparts because of their high specific surface area. Electrophoretic deposition (EPD) technique is a cost-effective, fast, versatile, and easy to perform method to fabricate porous nanoparticle films. However, conventional EPD is currently limited by the fact that the deposition rate decreases with time, resulting in an eventual plateau in the deposit yield. Here, we sought to overcome this limitation by establishing and leveraging the critical role of the particle's electrophoretic mobility in EPD kinetics.

Experiments: To identify the impact of electrophoretic mobility on EPD yield we used alumina nanoparticles suspended in ethanol as a model system. Changes in particle mobility were monitored via changes in the effective pH (pHe) of the suspension during EPD. We also developed a new suspension replenish EPD approach that allows us to maintain near-constant particle mobility and particle concentration with time thereby increasing yield.

Findings: We observed that in conventional EPD the particle mobility of the alumina nanoparticles decreased with time, resulting in a halting of deposition. Further, using the suspension replenish EPD, we observed a linear increase in the mass of the deposited film with time, overcoming the plateau limitation of conventional EPD.

Abbreviations: EPD, electrophoretic deposition; m, mass deposited; *f*, sticking parameter; C_s, particle concentration; μ, particle's electrophoretic mobility; A, area of the substrate; E, applied electric field; t, deposition time; pHe, effective pH; SEM, scanning electron microscope; HCl, hydrochloric acid; vol%, volume.

* Corresponding author at: University of Florida, 100 Rhines Hall, Gainesville, Florida 32611-6400, United States.
E-mail addresses: prabal.tiwari93@gmail.com (P. Tiwari), noah.ferson@ufl.edu (N.D. Ferson), jandrew@mse.ufl.edu (J.S. Andrew).

https://doi.org/10.1016/j.jcis.2020.02.103
0021-9797/

1. Introduction

The performance and sensitivity of catalyst, chemical, gas, and bio- sensing materials relies on the adsorption or transfer of matter (e.g., gases, chemicals, electrons, ions, or other analytes) on the surface or across the interface of the material. Thus, one approach to increase the performance and sensitivity of these materials is to increase their specific surface area (surface area per unit mass) [1–6]. Porous materials have higher specific surface area than their non-porous counterparts. There are various top-down and bottom-up approaches that can be used to fabricate porous materials. Top-down approaches include electrochemical etching of bulk materials and lithography while bottom-up approaches include self-assembly, drop-casting, spin coating, and electrophoretic deposition (EPD) of nanomaterials [1,7]. EPD has certain advantages over other top-down and bottom-up approaches such as relative ease, versatility in material choice, range of achievable thickness, cost-effectiveness, and faster rate of deposition [7–11]. However, EPD is plagued by several limitations, such as poor morphology control, poor adhesion of films, and a decrease in the deposition rate with time [12–17]. EPD deposits charged micro- and/or nano- particles suspended in a solution onto an oppositely charged electrode or substrate under the influence of an externally applied electric field. In this work, we seek to develop an EPD method that exhibits a constant deposition rate with time, overcoming limitations of existing methods by understanding the critical role of particle's electrophoretic mobility in this dynamic process.

Various factors determine the deposition rate (dm/dt) in EPD as shown by the first kinetic model developed by Hamaker:

$$dm/dt = f C_s \mu A E, \quad (1)$$

here, the deposition rate (dm/dt) is directly proportional to the sticking parameter (f), particle concentration (C_s), electrophoretic mobility of the particle (μ), area of the substrate (A), and electric field (E) [18]. However, this model fails to consider that these variables are time varying. For example, as the particles are deposited onto the substrate, it follows that the particle concentration (C_s) in the suspension decreases. It has also been experimentally shown that the effective electric field i.e., the electric field that the particles experience in the suspension also decreases with time despite a constant externally applied electric field [17,19,20]. This decrease in the effective electric field arises as the deposited film increases the resistance of the substrate [12,21]. Subsequently, Sarkar et al. developed a kinetic model that accounted for the time-variance of both particle concentration and effective electric field [12]. Based on the existing models, it is widely accepted that the decrease in deposition rate with time is due to these two time-decreasing factors i.e., particle concentration and effective electric field [7,14].

In this work, we demonstrate that the particle's electrophoretic mobility is another important factor driving the decrease in the deposition rate with time. The electrophoretic mobility determines how fast a particle moves under the influence of an electric field. The particle mobility is dependent on the surface charge which is a function of the pH of the suspension for an electrostatically stabilized particle [22]. The existing kinetic models assume that the particle mobility remains constant during deposition [14]. Contrary to that assumption, we showed that the particle mobility does not remain constant throughout deposition and decreases with time as the pH of suspension shifts towards the isoelectric point. Accordingly, this decrease in particle mobility with time should result in a corresponding decrease in the deposition rate (Eq. (1)). To demonstrate this relationship and its impact on deposition rate, we developed a set of experiments that would allow for the isolation of the effect of the particle mobility on the EPD yield. Fig. 1 shows our particle replenish approach, which was used to keep the particle concentration and the effective electric field nearly constant with time while allowing the particle mobility to vary with time. This allowed us to isolate the role of the time-decreasing particle mobility on the deposition rate.

Further, with an understanding of the critical role that the particle mobility plays in determining the EPD yield, we developed a suspension replenish EPD approach in which a fresh suspension was introduced at every 10 min interval, replenishing both the particle mobility and the particle concentration back to their original values. As a result, we obtained a constant deposition rate with time overcoming the plateau limitation faced in conventional EPD, achieving up to 6 times improvement in both the yield and the thickness of the deposit. We anticipate that this approach is broadly applicable to a wide variety of materials and can be used to manufacture various electronic and medical devices from nanomaterials in a more efficient and scalable manner.

2. Experimental section

2.1. Initial stable suspension preparation

Dry α-alumina nanoparticles (>99% purity, 80 nm diameter, 3.97 g/cm^3 density) were purchased from US Research Nanomaterials, Inc., USA. A non-aqueous solvent (200 proof ethanol, Acros Organics) was used to prepare the initial suspensions. α-alumina nanoparticles were added to a 20 ml solution of hydrochloric acid (Technical HCl, Fischer Chemical) and ethanol to obtain a positively charged suspension of 0.25 vol% (vol.%) alumina nanoparticles. The initial suspension had an effective pHe of ~ 1.70 +/- 0.04. A Branson SFX 550 probe ultra-sonicator with a 1/4th – inch micro-trip attachment was used in the pulse mode (20 s on and 10 s off) for 3 min at an amplitude of 18% to break up particle agglomerates in the suspensions. During ultra-sonication, the suspension was contained in a 50 ml centrifuge tube which was surrounded by an ice water bath to prevent heating of the suspension.

2.2. Suspension characterization

Operational pH measurements were performed in non-aqueous solvents and are referred to as the effective pH or pHe [23,24]. The pHe measurements were performed according to the ASTM D6423-19 standard protocol using a Thermo Scientific 5107 BNMD No-Cal pH/Automated Temperature Compensation combination electrode connected to a Thermo Scientific Orion Star A111 benchtop pH meter [23]. The pH electrode was calibrated using fresh Thermo Scientific buffers (pH 1.68, pH 4.01, and pH 7.00) before each measurement unless the measurements were performed on the same day. The suspensions were poured into a 20 ml borosilicate beaker and magnetically stirred during the measurement. The pH probe was immersed in the stirred suspensions and the pHe values were recorded 30 s after immersion. The zeta potential and the electrophoretic particle mobility of alumina particles in solution were measured using Malvern Panalytical's Zetasizer Ultra instrument. Malvern's diffusion barrier technique was used to perform these measurements. The zeta potential was calculated from the particle mobility using the Hückel model.

2.3. Electrophoretic deposition of nanoparticles

In this work, three electrophoretic deposition variants were performed, including conventional EPD, particle replenish EPD, and suspension replenish EPD. All three EPD variants were performed using a Bio-Rad Power-Pac 1000 power supply in

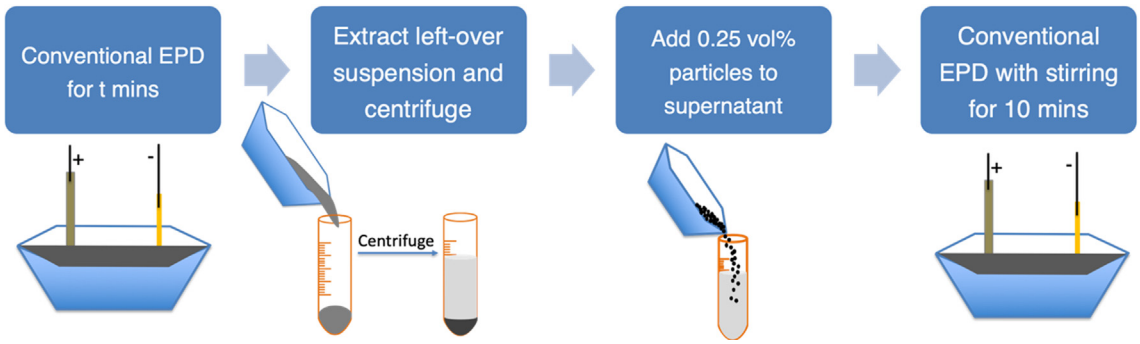

Fig. 1. Flow-chart diagram of particle replenish EPD.

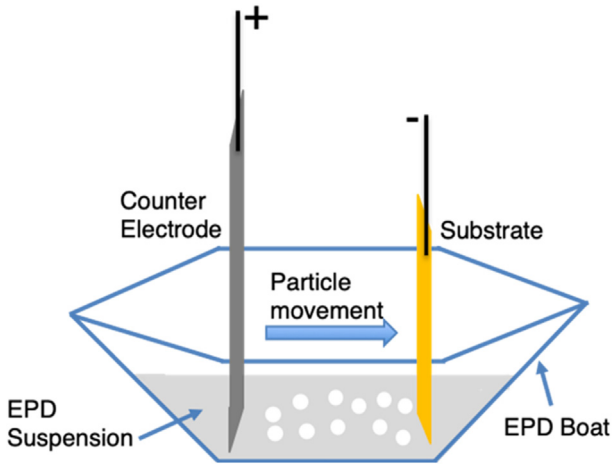

Fig. 2. Schematic of the electrophoretic deposition (EPD) set up used for all depositions.

constant-voltage mode. A schematic of the setup used for all depositions is shown in Fig. 2. A Fisherbrand hexagonal polystyrene weigh boat of 47 mm inner diameter sitting on a lab jack (stage) was used to contain the EPD suspensions. Compressible graphite (7.50 mm wide × 35.50 mm long × 3.00 mm thick) was used as the counter electrode and was connected to the positive terminal of the power supply using an alligator clip. Substrates were fabricated by sputtering 10 nm of titanium (adhesion layer) onto a 4-inch ⟨1 0 0⟩ prime-grade silicon wafer followed by sputtering a 100 nm gold layer onto the titanium layer using a KJL CMS-18 Multi-Source sputtering tool in a cleanroom facility. The wafer was then diced into 6 mm × 20 mm substrates using an ADT 7100 dicing saw. Before EPD, the substrates were cleaned using isopropyl alcohol and deionized water, followed by drying with nitrogen gas. After cleaning and drying, the initial weight of the substrate was measured using an analytical balance. The substrate was then connected to the negative terminal of the power supply using an alligator clip and kept parallel and 33 mm from the counter electrode. The bottom edge of the substrate and the counter electrode were kept ~1 mm above the bottom of the weigh boat.

2.3.1. Conventional electrophoretic deposition

In conventional EPD, depositions were performed for 10, 30, 50, and 70 min with applied electric fields of 20, 40, 60, 80, and 100 V/cm. After each deposition, the power was turned off, and the counter electrode and the substrate were removed from the suspension by moving the stage down. The as-deposited film was then dried in air for 3 min before the mass measurement. To visualize the pHe of different regions in the EPD suspension after the deposition, a universal pH indicator solution by Ricca Chemicals was used. 500 μL of the indicator solution was pipetted into the EPD suspension after the power was turned off and the photographs of the EPD suspension were taken after the color change had equilibrated (~1 min). To determine the pHe of the solution from the color of the universal indicator solution a reference chart (Supplementary Fig. S1) was prepared by adding hydrochloric acid/sodium hydroxide to ethanol.

2.3.2. Particle replenish electrophoretic deposition

To maintain the particle concentration and the effective electric field nearly constant with time to let only particle mobility vary with time, particle replenish EPD (Fig. 1) was developed. In this approach, first, conventional EPDs were performed for 10, 20, and 30 min with an applied electric field of 100 V/cm. After the depositions, the used suspensions were collected from the EPD boat and poured into 50 ml centrifuge tubes. The collected suspensions were centrifuged at 9000 RPM for 10 min using an Eppendorf 5804 centrifuge to separate the supernatant from the particles. The supernatant solutions were then transferred to fresh 50 ml centrifuge tubes using a pipette. Fresh α-alumina nanoparticles were then added to 20 ml of the supernatant solutions to obtain the initial particle concentration of 0.25 vol%, replenishing the particle concentration back to the original concentration. Each of the particle replenished EPD suspensions were then used to perform a conventional EPD for 10 min with an applied field of 100 V/cm. The suspension was also magnetically stirred during deposition to further maintain constant particle concentration. A fresh substrate was used for each deposition to maintain a near constant effective electric field. After each deposition, the film was removed from the suspension and air-dried for 3 min prior to mass measurement.

2.3.3. Suspension replenish electrophoretic deposition

In suspension replenish EPD, deposition was paused after every 10 min to remove the old suspension, followed by the introduction of a fresh suspension and resumption of deposition for another 10 min. These steps were repeated until a total deposition time of 30, 50, and 70 min was obtained for applied electric fields of 20 V/cm and 100 V/cm. After each deposition, the film was removed from the suspension and air-dried for 3 min prior to mass measurement.

2.3.4. Characterization of electrophoretic deposition films

Scanning electron microscopy (SEM) images of cross-sections of the deposited films were taken using an FEI Nova NanoSEM 430 to determine the film thickness. The cross-sections of the deposited films were prepared by cleaving the samples using a tungsten scribe. Before performing SEM, the cleaved samples were coated with a 10 nm conductive layer of gold–palladium using a Denton

Desk 2 sputter coater. The film thickness was measured from the SEM images using ImageJ.

3. Results and discussion

3.1. Conventional electrophoretic deposition kinetics

Fig. 3 shows the mass of the deposited film as a function of the deposition time in conventional EPD for applied electric fields ranging from 20 to 100 V/cm. In each of these depositions, the deposition rate, i.e., slope, decreases with time, and the yield ultimately plateaus after approximately 30 min. The current EPD kinetics models attribute this effect to a decrease in both the particle concentration and the effective electric field in the suspension with the increasing deposition time [12,14]. However, we hypothesize that the electrophoretic mobility of the particle is also decreasing with time and may also contribute to this plateau in yield. The existing models have assumed that the particle mobility remains constant during EPD.

During EPD, the pH or effective pH (pHe, for non-aqueous solvents) of the suspension will change. This pH changes arises because the hydrogen ions in the solution undergo an electrochemical reaction, forming H_2 gas upon gaining electrons from the negative electrode. This depletion of H^+ ions causes the pH or the effective pH (pHe, for non-aqueous solvents) of the suspension to change. This change in pH/pHe will also affect the surface chemistry of an oxide particle as its surface is protonated or deprotonated, thereby changing its surface charge and its electrophoretic mobility [22,25]. To show that the pH/pHe of the EPD suspension is changing as a function of time, a universal indicator solution was added to the EPD suspension after 10, 30, 50 and 70 min of deposition (non-stirred) performed with an applied electric field of 100 V/cm (Fig. 4). Fig. 4a shows that after 10 min the suspension has a uniform pHe of approximately 2, which is close to the initial value. However, after 30 min of deposition (Fig. 4b), the pHe of the suspension is no longer uniform and the pHe near the substrate is much higher, indicated by the bluish-green color (pHe ~ 10–13). This local pHe rise near the substrate can be attributed to the depletion/electrochemical reduction of H^+ ions occurring at the negatively charged substrate. After 50 min of deposition (Fig. 4c), the color of the bulk of the suspension has shifted to yellow corresponding to pHe of approximately 10. Moreover, the region of the suspension near the substrate that has shifted to a basic pHe extends further into the suspension. The isoelectric point of alumina is ~pH 9 [25]. Thus, as the EPD experiment continues, the pHe of the suspension near the substrate shifts towards this value, where the alumina particles will have zero electrophoretic mobility, and thus not be mobile in an applied E-field. Additionally, the time of 30 min, where there is an observable pHe shift near the substrate to the isoelectric point of the alumina particles corresponds to the time when a significant drop in the deposition rate is observed in Fig. 3. Thus, the decreasing particle mobility with time is likely also contributing to the plateau in yield with increasing deposition time. This shift of pH/pHe of suspension towards the isoelectric point of the suspended particle is also reported in other EPD studies [19,26-31]. We also observed that upon continuous stirring of suspension during the deposition the pHe gradients were not visible but the pHe still shifts towards the isoelectric point of alumina with time as shown in Supplementary Fig. S2.

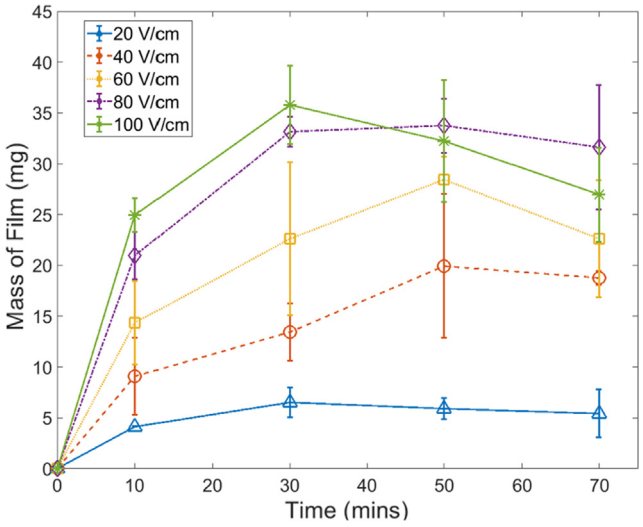

Fig. 3. The mass of the deposited film as a function of the deposition time for the films deposited via conventional EPD using applied electric fields ranging from 20 to 100 V/cm. For each data point, three EPD runs were performed, and their corresponding film mass was measured to calculate the average and the standard deviation. Lines are a guide to the eye.

3.2. Particle replenish electrophoretic deposition kinetics

Here, we hypothesize that the decrease in the particle mobility with time results in a decrease in the deposition rate and the ultimate plateau in yield. To confirm this statement, we developed a particle replenishment EPD method (Fig. 1) that allowed us to perform depositions where the particle concentration and the electric field in the suspension were maintained nearly constant with time to isolate the effect of the time-decreasing particle mobility on yield. In this method, supernatants from the conventional EPDs performed at 100 V/cm for 10, 20, and 30 min were collected via centrifugation. These supernatants were then used to suspend the initial concentration of particles (0.25 vol%). This allowed the pHe of the suspension to vary with time while allowing particle concentration to be nearly constant as it was replenished to the original value every 10 min. Each of the particle replenished EPD suspensions were then used to perform a conventional EPD for 10 min with an applied electric field of 100 V/cm. The suspension was also stirred during the deposition to minimize settling of the alumina particles to further promote maintaining a near-constant particle concentration. Additionally, when the suspension was

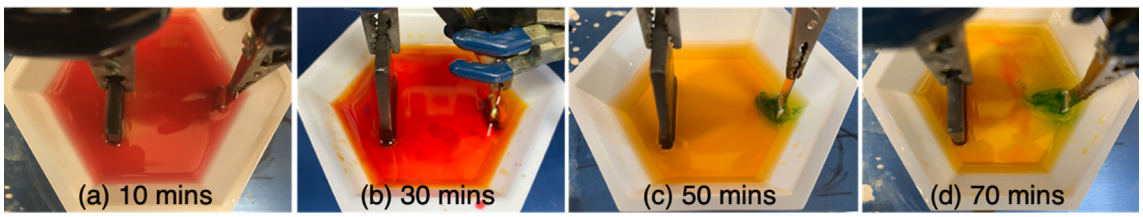

Fig. 4. Photographs of the EPD suspensions taken after adding universal pH indicator solution in them after (a) 10 min, (b) 30 min, (c) 50 min, and (d) 70 min of deposition (non-stirred) was performed with an electric field of 100 V/cm via conventional EPD. Red color represents pHe ~ 2, yellow color represents pHe ~ 10, and the bluish-green color represents pHe ~ 10–13.

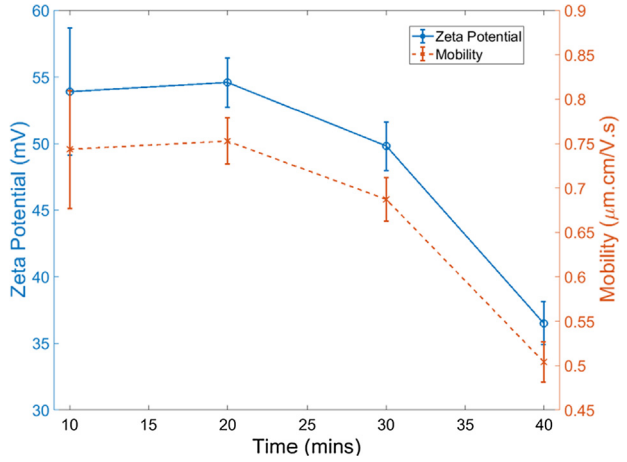

Fig. 5. The zeta potential and electrophoretic mobility of alumina particles plotted as a function of deposition time. For each data point, five measurements were performed to calculate the average and the standard deviation (error bars). Lines are a guide to the eye.

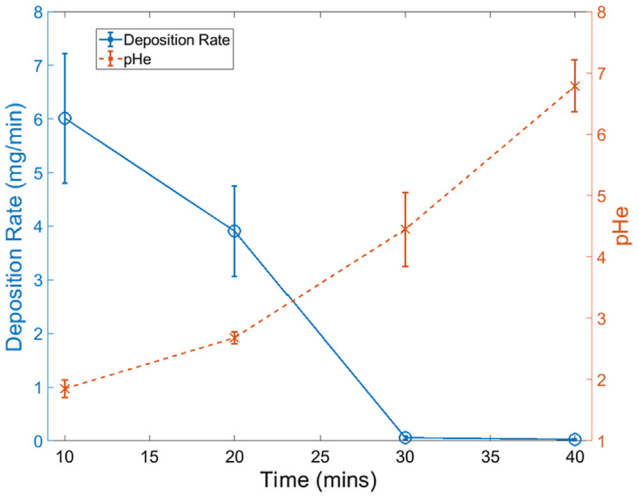

Fig. 6. The deposition rate and the pHe of the suspension as a function of the deposition time. The deposition rate was obtained by running EPDs at 100 V/cm and the particle concentration and substrates were replenished at every 10 min interval. For each data point, three experiment repeats were performed to calculate the average and the standard deviation (error bars). Lines are a guide to the eye.

replenished to the initial particle concentration a fresh substrate was also utilized for the deposition so the effective electric field would also be maintained near-constant with time. Therefore, in this particle replenish EPD, the only deposition parameter that is changing with time is the pHe of the suspension, and thereby the particle mobility. The trend of particle mobility and zeta potential as a function of deposition time is plotted in Fig. 5. It shows that both zeta potential and particle mobility are decreasing as a function of deposition time as expected.

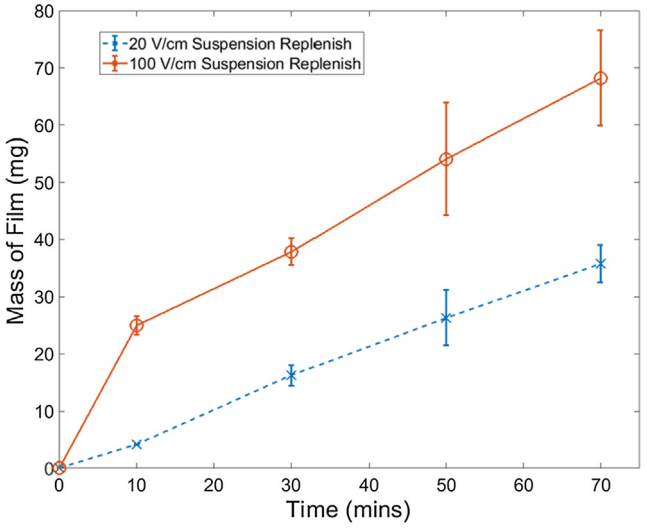

Fig. 7. The mass of the deposited film as a function of the deposition time deposited via suspension replenish EPD by applying 20 V/cm and 100 V/cm fields. For each field and time condition, three EPD runs were performed, and their corresponding film mass was measured to calculate the average mass of the film. The error bars correspond to the standard deviation amongst the three runs. Lines are a guide to the eye.

Furthermore, Fig. 6 proves our hypothesis and shows that the deposition rate drops as a function of time as the pHe of the suspension increases and the particle mobility decreases. Similar to what was seen for conventional EPD, Figs. 3 and 4, the deposition rate drops off significantly after 30 min. These results suggest that decreasing particle mobility is another factor causing the decrease in the EPD deposition rate with increased deposition time.

3.3. Suspension replenish electrophoretic deposition

In the previous section, we established that particle mobility plays a critical role in the decreasing deposition rate with time. Therefore, we hypothesized that we can overcome the plateau limitation of conventional EPD by developing a suspension replenish EPD approach in which both the particle mobility and the particle concentration were maintained nearly constant with time by the

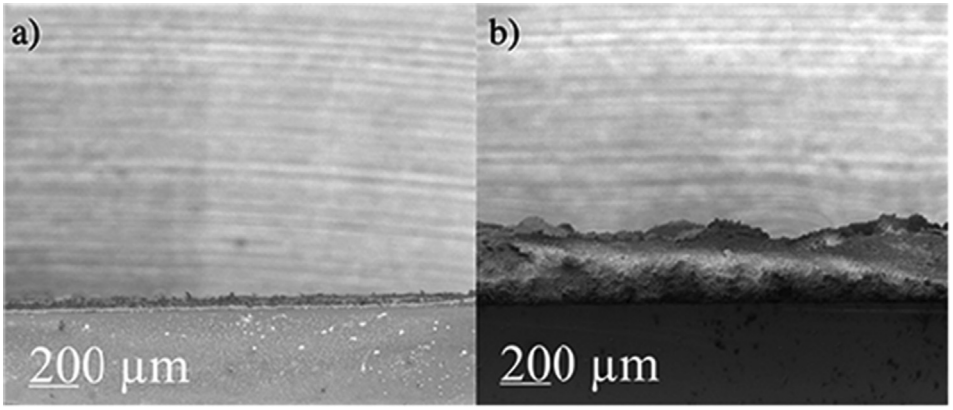

Fig. 8. Cross-sectional SEM of the films deposited via (a) conventional EPD and (b) suspension replenish EPD, both deposited at 20 V/cm for 70 min. The average thickness of conventional EPD film is 54.40 μm +/- 5.90 μm, while, the average thickness of the suspension replenish EPD film is 304.30 μm +/- 28.80 μm.

replenishment of the suspension at 10 min intervals. Fig. 7 shows that that the mass of the deposited film keeps increasing with time for both 20 V/cm and 100 V/cm up to 70 min without encountering the plateau of conventional EPD (Fig. 3). Thus, we showed that the plateau limitation of conventional EPD can be overcome by maintaining constant particle mobility and particle concentration during the deposition. Additionally, the cross-sectional SEM images of the films (Fig. 8) show that the film deposited via suspension replenish EPD is 6 times thicker (304.30 μm +/− 28.80 μm) than that deposited via conventional EPD (54.40 μm +/− 5.90 μm) using the same electric field and time conditions. Moreover, the yield of this suspension replenish EPD film is also 6 times greater (35.76 +/− 3.26 mg) than the conventional EPD film (5.44 +/− 2.34 mg). It is important to note that improvement in yield can also be obtained by adjusting the pH of the suspension back to original via titration to replenish the particle mobility. One advantage of this technique is that it would consume less material compared to the suspension replenish approach.

4. Conclusions

Conventional EPD suffers from a major limitation, whereby the deposition rate decreases with time and causes the deposit yield to eventually plateau [7,12,14,32,33]. The existing EPD kinetic models attribute this effect to a decrease in the particle concentration and the effective electric field with time [12,14]. These models assume that the particle's electrophoretic mobility remains constant with time and does not affect the deposition rate kinetics. Contrary to that assumption, we showed that the particle mobility does decrease with time and significantly decreases the deposition rate. Using α-alumina nanoparticles suspended in ethanol as a model system, we showed that pHe of the suspension shifts towards the isoelectric point of alumina during EPD. This pHe shift towards the isoelectric point causes a significant decrease in the particle mobility. By developing a particle replenish EPD approach, we isolated the effect of the time-decreasing particle mobility on yield as both the particle concentration and the effective electric field were maintained nearly constant with time and only the particle mobility was decreasing with time. As a consequence of the time-decreasing particle mobility, we saw that the deposition rate dropped to 0 mg/min after only 30 min of deposition. Furthermore, utilizing this knowledge we overcame the plateau limitation of conventional EPD by developing a suspension replenish EPD approach in which both the particle mobility and the particle concentration were maintained nearly constant with time. Using this approach, we observed a constant deposition rate with time and the yield kept increasing with time overcoming the plateau limitation of conventional EPD [7,17,32]. It led to up to 6 times improvement in both the yield and the thickness of the deposit. Since this approach applies to a wide variety of materials which are electrostatically stabilized using pH adjustment, the yield and the thickness of deposits of a number of materials can be improved significantly by using the suspension replenish electrophoretic deposition approach.

CRediT authorship contribution statement

Prabal Tiwari: Conceptualization, Methodology, Formal analysis, Investigation, Visualization. **Noah D. Ferson:** Methodology, Formal analysis, Visualization. **Jennifer S. Andrew:** Conceptualization, Methodology, Formal analysis, Supervision.

Declaration of Competing Interest

The authors declare that they have no known competing financial interests or personal relationships that could have appeared to influence the work reported in this paper.

Acknowledgements

This work was supported by the National Science Foundation through the Scalable Nanomanufacturing Program, Award No. CMMI-1727930.

Appendix A. Supplementary material

Supplementary data to this article can be found online at https://doi.org/10.1016/j.jcis.2020.02.103.

References

[1] T. Wagner, S. Haffer, C. Weinberger, D. Klaus, M. Tiemann, Mesoporous materials as gas sensors, Chem. Soc. Rev. 42 (2013) 4036–4053.
[2] M. Tiemann, Porous metal oxides as gas sensors, Chem. Eur. J. 13 (2007) 8376–8388.
[3] G. Jasiński, P. Jasiński, B. Chachulski, Nano-porous alumina humidity sensors, Metrol. Meas. Syst. 15 (2008) 195–204.
[4] V. Timár-Horváth, L. Juhász, A. Vass-Várnai, G. Perlaky, Usage of porous Al2O3layers for RH sensing, Microsyst. Technol. 14 (2008) 1081–1086, https://doi.org/10.1007/s00542-007-0466-2.
[5] T. Ishihara, S. Matsubara, Capacitive type gas sensors, J. Electroceramics. 2 (1998) 215–228.
[6] C. Wang, L. Yin, L. Zhang, D. Xiang, R. Gao, Metal oxide gas sensors: sensitivity and influencing factors, Sensors 10 (2010) 2088–2106.
[7] L. Besra, M. Liu, A review on fundamentals and applications of electrophoretic deposition (EPD), Prog. Mater Sci. 52 (2007) 1–61, https://doi.org/10.1016/j.pmatsci.2006.07.001.
[8] S.J. Kelly, X. Wen, D.P. Arnold, J.S. Andrew, Electrophoretic deposition of nickel zinc ferrite nanoparticles into microstructured patterns, AIP Adv. 6 (2016), https://doi.org/10.1063/1.4943150.
[9] L. Vogt, M. Schäfer, D. Kurth, F. Raether, Usability of electrophoretic deposition for additive manufacturing of ceramics, Ceram. Int. (2019), https://doi.org/10.1016/j.ceramint.2019.04.129.
[10] I. Zhitomirsky, Cathodic electrodeposition of ceramic and organoceramic materials. Fundamental aspects, Adv. Colloid Interface Sci. 97 (2002) 279–317, https://doi.org/10.1016/S0001-8686(01)00068-9.
[11] J.H. Dickerson, A.R. Boccaccini, Electrophoretic deposition of nanomaterials, Springer, 2011.
[12] P. Sarkar, P.S. Nicholson, Electrophoretic deposition (EPD): Mechanisms, kinetics, and application to ceramics, J. Am. Ceram. Soc. 79 (1996) 1987–2002, https://doi.org/10.1111/j.1151-2916.1996.tb08929.x.
[13] O.O. Van Der Biest, L.J. Vandeperre, Electrophoretic deposition, Membr. Technol. 2002 (2002) 13, https://doi.org/10.1016/S0958-2118(02)80166-5.
[14] B. Ferrari, R. Moreno, EPD kinetics: A review, J. Eur. Ceram. Soc. 30 (2010) 1069–1078, https://doi.org/10.1016/j.jeurceramsoc.2009.08.022.
[15] A.R. Boccaccini, S. Keim, R. Ma, Y. Li, I. Zhitomirsky, Electrophoretic deposition of biomaterials, J. R. Soc. Interface 7 (2010), https://doi.org/10.1098/rsif.2010.0156.focus.
[16] I. Corni, M.P. Ryan, A.R. Boccaccini, Electrophoretic deposition: From traditional ceramics to nanotechnology, J. Eur. Ceram. Soc. 28 (2008) 1353–1367, https://doi.org/10.1016/J.JEURCERAMSOC.2007.12.011.
[17] Y.C. Wang, I.C. Leu, M.H. Hon, Kinetics of electrophoretic deposition for nanocrystalline zinc oxide coatings, J. Am. Ceram. Soc. 87 (2004) 84–88, https://doi.org/10.1111/j.1551-2916.2004.00084.x.
[18] B.H. C Hamaker, FORMATION O F A DEPOSIT BY ELECTRO-PHORESIS, n.d. https://pubs.rsc.org/en/content/articlepdf/1940/tf/tf9403500279 (accessed November 15, 2018).
[19] L. Stappers, L. Zhang, O. Van der Biest, J. Fransaer, The effect of electrolyte conductivity on electrophoretic deposition, J. Colloid Interface Sci. 328 (2008) 436–446, https://doi.org/10.1016/j.jcis.2008.09.022.
[20] G. Anné, K. Vanmeensel, J. Vleugels, O. Van Der Biest, Influence of the suspension composition on the electric field and deposition rate during electrophoretic deposition, Colloids Surf. A Physicochem. Eng. Asp. 245 (2004) 35–39, https://doi.org/10.1016/j.colsurfa.2004.07.001.
[21] O. Van Der Biest, S. Put, G. Anné, J. Vleugels, Electrophoretic deposition for coatings and free standing objects, J. Mater. Sci. 39 (2004) 779–785, https://doi.org/10.1023/B:JMSC.0000012905.62256.39.
[22] R.J. Hunter, Foundations of colloid science, Oxford University Press, 2001.
[23] E. Fuel, A.S. Engines, Standard Test Method for Determination of pHe of Ethanol , Denatured Fuel Ethanol, and Fuel Ethanol (Ed75-Ed85) 1, Readings. (1999) 4–6. doi:10.1520/D6423-14.2.
[24] Thermo Scientific, Measuring pH of non-aqueous and mixed samples, Thermo Fischer Sci. (2014).
[25] G.V. Franks, Y. Gan, Charging behavior at the alumina-water interface and implications for ceramic processing, J. Am. Ceram. Soc. 90 (2007) 3373–3388, https://doi.org/10.1111/j.1551-2916.2007.02013.x.
[26] R.J. Kershner, J.W. Bullard, M.J. Cima, The role of electrochemical reactions during electrophoretic particle deposition, J. Colloid Interface Sci. 278 (2004) 146–154, https://doi.org/10.1016/j.jcis.2004.05.017.

[27] M. Mishra, Y. Sakka, T. Uchikoshi, L. Besra, pH localization: a case study during electrophoretic deposition of ternary MAX phase carbide-Ti3SiC2, J. Ceram. Soc. Japan. 121 (2013) 348–354, https://doi.org/10.2109/jcersj2.121.348.
[28] L. Besra, T. Uchikoshi, T.S. Suzuki, Y. Sakka, Experimental verification of pH localization mechanism of particle consolidation at the electrode/solution interface and its application to pulsed DC electrophoretic deposition (EPD), J. Eur. Ceram. Soc. 30 (2010) 1187–1193.
[29] M. Mishra, S. Bhattacharjee, L. Besra, H.S. Sharma, T. Uchikoshi, Y. Sakka, Effect of pH localization on microstructure evolution of deposits during aqueous electrophoretic deposition (EPD), J. Eur. Ceram. Soc. 30 (2010) 2467–2473, https://doi.org/10.1016/j.jeurceramsoc.2010.04.034.
[30] A.T. Kuhn, C.Y. Chan, pH changes at near-electrode surfaces, J. Appl. Electrochem. 13 (1983) 189–207, https://doi.org/10.1007/BF00612481.
[31] D. De, P.S. Nicholson, Role of ionic depletion in deposition during electrophoretic deposition, J. Am. Ceram. Soc. 82 (2004) 3031–3036, https://doi.org/10.1111/j.1151-2916.1999.tb02198.x.
[32] A.R. Boccaccini, J.H. Dickerson, Electrophoretic deposition: Fundamentals and applications, J. Phys. Chem. B 117 (2013) 1501, https://doi.org/10.1021/jp211212y.
[33] O.O. Van der Biest, L.J. Vandeperre, Electrophoretic deposition of materials, Annu. Rev. Mater. Sci. 29 (1999) 327–352.